Dithiothreitol Activity by Particulate Oxidizers of SOA Produced from Photooxidation of Hydrocarbons under Varied NO$_x$ Levels

Huanhuan Jiang,[1] Myoseon Jang,[1] Zechen Yu,[1]

[1]Department of Environmental Engineering Sciences, Engineering School of Sustainable Infrastructure and
5   Environment, University of Florida, Gainesville, FL 32608, USA

Correspondence to: Myoseon Jang (mjang@ufl.edu)

Abstract. When hydrocarbons are atmospherically oxidized, they form particulate oxidizers, including quinones, organic hydroperoxides, and peroxyacyl nitrates (PANs). These particulate oxidizers can modify cellular materials (e.g., proteins and enzymes), and adversely modulate cell

10 functions. In this study, the contribution of particulate oxidizers in secondary organic aerosols (SOA) to the oxidative potential was investigated. SOA were generated from the photooxidation of toluene, 1,3,5-trimethylbenzene, isoprene, and α-pinene under varied NO$_x$ levels. Oxidative potential was determined from the typical mass-normalized consumption rate (reaction time $t = 30$ min) of dithiothreitol (DTT$_t$), a surrogate for biological reducing agents. At high NO$_x$ conditions,

15 the DTT$_t$ of toluene SOA was 2–5 times higher than that of the other types of SOA. Isoprene DTT$_t$ significantly decreased with increasing NO$_x$ (up to 69 % reduction by changing the hydrocarbon/NO$_x$ ratio from 30 to 5). The DTT$_t$ of 1,3,5-trimethylbenzene and α-pinene SOA was insensitive to NO$_x$ under the experimental conditions of this study. The significance of quinones to the oxidative potential of SOA was tested through the enhancement of DTT consumption in the

20 presence of 2,4-dimethylimidazole, a co-catalyst for the redox cycling of quinones; however, no significant effect of 2,4-dimethylimidazole on modulation of DTT consumption was observed for all SOA, suggesting that a negligible amount of quinones was present in SOA of this study. For toluene and isoprene, mass-normalized DTT consumption (DTT$_m$) was determined over an extended period of reaction time ($t = 2$ h) to quantify their maximum capacity to consume DTT.

25 The total quantities of PANs and organic hydroperoxides in toluene SOA and isoprene SOA were also measured using the Griess assay and the 4-nitrophenylboronic acid assay, respectively. Under the NO$_x$ conditions (HC/NO$_x$ ratio: 5-36 ppbC/ppb) applied in this study, the amount of organic hydroperoxides was substantial, while PANs were found to be insignificant for both SOA. Isoprene DTT$_m$ was almost exclusively attributable to organic hydroperoxides, while toluene

30 DTT$_m$ was partially attributable to organic hydroperoxides. The DTT assay results of the model

compound study suggested that electron-deficient alkenes, which are abundant in toluene SOA, could also modulate DTT_m.

1 Introduction

Epidemiological studies have linked human exposure to fine particulate matter ($PM_{2.5}$, aerodynamic diameter < 2.5 μm) to increased morbidity and mortality from respiratory and cardiovascular diseases (e.g., asthma, myocardial infarction, stroke) (Brook et al., 2010; Chen et al., 2013; Davidson et al., 2005; Jansen et al., 2005; Katsouyanni et al., 1997; van Eeden et al., 2005). Primary combustion particulates (e.g., wood smoke particles, vehicle emissions) are known to be causative agents of these diseases (Danielsen et al., 2011; Nel, 2005); however, increasing attention is also being paid to secondary organic aerosols (SOA) (Fujitani et al., 2012; Jang et al., 2006; Kramer et al., 2016; Lin et al., 2016; McDonald et al., 2010; McWhinney et al., 2013; Tuet et al., 2017a; Tuet et al., 2017b), which are produced from the atmospheric transformation of hydrocarbons (HCs) in the presence of atmospheric oxidants (e.g., NO_x, OH radicals, O_3) (Hallquist et al., 2009). Although SOA comprises a large fraction of $PM_{2.5}$ (20–90 %) (Gelencsér et al., 2007; Kanakidou et al., 2005), its mechanistic role in causing adverse health effects remains unclear.

The toxicity of organic aerosols has been ascribed to the generation of reactive oxygen species (ROS) and the modification of biomolecules (e.g., DNA and cellular enzymes) (Danielsen et al., 2011; Nel, 2005). ROS can induce oxidative stress in pulmonary systems, followed by a cascade of inflammation responses, and ultimately the apoptosis of lung cells (Danielsen et al., 2011; Li et al., 2003; Li et al., 2008). Particulate organic compounds such as quinones and polyaromatic hydrocarbons can react with cellular reducing agents (e.g., NADPH) and form ROS (i.e., H_2O_2 and $O_2^{\cdot-}$) (Kumagai et al., 2012). To efficiently determine the oxidative potential (the ability to generate ROS) of different types of particulate matter at a laboratory benchtop scale, a low-cost acellular technique, dithiothreitol (DTT) assay, has been widely used (Antiñolo et al., 2015; Cho et al., 2005; Hedayat et al., 2014; Janssen et al., 2014; Kramer et al., 2016; Verma et al., 2015). DTT acts as a surrogate for biological reducing agents owing to its two sulfhydryl groups. A recent study by Tuet et al. (Tuet et al., 2017a) has reported a positive nonlinear correlation between DTT activities and ROS production in murine alveolar macrophages. Some quinones (e.g., 1,4-naphthoquinone (NQN) and 9,10-phenathraquinone (PQN)) can efficiently consume DTT via a

catalytic redox cycle, during which quinones are reduced to semiquinones or hydroquinones (Chung et al., 2006; Li et al., 2003). Hence, quinone compounds, commonly found in primary combustion particulates (Danielsen et al., 2011; Jakober et al., 2007), are known to be important contributors to DTT response of combustion particles.

5 Unlike combustion PM, biogenic SOA and most aromatic SOA (except naphthalene SOA) contain little or no quinones (Forstner et al., 1997; Hamilton et al., 2005; McWhinney et al., 2013; Pindado Jiménez et al., 2013); however, recent work has shown that the DTT activity of SOA (toluene, 1,3,5-trimethylbenzene (TMB), isoprene, and α-pinene) was high and even comparable to that originating from combustion particulates (e.g., wood smoke particles) (Jiang et al., 2016),

10 suggesting that there must be unidentified mechanisms underlying DTT consumption other than the catalytic act of quinones.

In this study, three groups of SOA products were introduced to explain the mechanistic role of SOA products in DTT consumption (Fig. 1a and 1b). First, non-catalytic particulate oxidizers in SOA, such as organic hydroperoxides (alkyl hydroperoxides and acyl hydroperoxides) and peroxy

15 acyl nitrates ($RC(O)OONO_2$; PANs), can oxidize sulfhydryl groups in DTT to form disulfides, sulfenic acids (RSOH), sulfinic acids (RSO_2H), or sulfonic acids (RSO_3H) (Grek et al., 2013; Mudd, 1966). These non-catalytic particulate oxidizers are abundant in SOA sourced from various hydrocarbons (Docherty et al., 2005; Sato et al., 2012). Second, catalytic particulate oxidizers, such as quinoid substances, can oxidize sulfhydryl groups through a redox cycle (Cho et al., 2005;

20 Kumagai et al., 2002). A trace amount of quinones can be found in aromatic SOA products (Forstner et al., 1997). Third, electron-deficient alkenes in SOA can react with the sulfhydryl groups of DTT via a Michael addition (Nair et al., 2014). Alkenes substituted with an electron withdrawing group (e.g., conjugated carbonyls) are commonly found in ring-opening products from the photooxidation of aromatic HCs (e.g., toluene) (Jang and Kamens, 2001; Saunders et al.,

25 2003, 1997; Wyche et al., 2009). The contributions of all three groups of SOA products to DTT activity can be influenced by the type of precursor HC (aromatics vs. biogenics) and by NO_x ($NO+NO_2$) levels (HC/NO_x ratios) (Eddingsaas et al., 2012b; Jang and Kamens, 2001; Wyche et al., 2009; Xu et al., 2014).

Advanced analytical instruments (e.g., aerosol mass spectrometers and liquid chromatograph mass

30 spectrometers integrated with soft ionization) have innovated the characterization of SOA compositions; however, their data are limited to elemental analysis (Xu et al., 2014) or the

identification of some chemical species (e.g., carboxylic acids and carbonyls) by a unique fragmentation (Sato et al., 2012; Shiraiwa et al., 2013). Particulate oxidizers (e.g., PANs and organic hydroperoxides) are thermally unstable and can decompose during chemical injection at high temperature, making it difficult to characterize SOA compositions using mass spectrometers

5 (Zheng et al., 2011). This difficulty is also compounded by a lack of authentic standards suitable for the analysis of diverse and complex particulate oxidizers.

The purpose of this study is to characterize the effect of SOA products on DTT consumption. SOA were generated from the photooxidation of different HCs under varied environmental conditions (NO_x levels) using a large outdoor photochemical smog chamber. The two most abundant

10 anthropogenic HCs (i.e., toluene and TMB) in the ambient atmosphere and the two ubiquitous biogenic HCs (i.e., isoprene and α-pinene) were chosen as SOA precursors. Aerosols were collected using an online technique with a particle-into-liquid sampler (PILS). Selected toluene and isoprene SOA samples were immediately applied to the DTT assay and the quantification of particulate oxidizers. The amount of PAN was measured using the Griess assay and that of organic

15 hydroperoxides was measured using the 4-nitrophenylboronic acid (NPBA) assay. The contribution of quinones to the oxidative potential of SOA was estimated by the enhancement of DTT consumption in the presence of 2,4-dimethylimidazole, a co-catalyst for the redox cycling of quinones (Dou et al., 2015). In addition to particulate oxidizers, the contribution of electron-deficient alkenes to DTT activity was investigated for aromatic SOA (toluene SOA). Although the

20 chemical assays (e.g., NPBA assay and Griess assay) used in this study have limitations (e.g., providing structural details of organic compounds), they are user-friendly and can accurately quantify the total amount of organic hydroperoxides and PANs, both of which are important for understanding the role of SOA in cellular oxidative stress at the molecular level. The quality control (QC) of the chemical assays used in this study will be discussed.

25 **2 Materials and methods**

2.1 Outdoor chamber experiments

SOA were generated under natural conditions (ambient sunlight, temperature, and relative humidity) using the University of Florida Atmospheric PHotochemical Outdoor Reactor (UF-APHOR) dual chambers (52 m^3 each). Before each experiment, the chambers were flushed with

the clean air for 2 days using an air purifier system (GC Series, IQAir Inc.) until the background particle mass concentration was below 1 μg m^{-3}. HC and NO (2% in N$_2$, Airgas) were injected to the chamber before sunrise. For photooxidation experiments of toluene, HONO generated from the reaction of 0.1 M NaNO$_2$ solution and 10 % w/w H$_2$SO$_4$ solution was injected into the chamber

5   as a source of OH radicals. HONO produced OH radicals and NO via photolysis. The particle size distribution of chamber SOA was monitored using a scanning mobility particle sizer (SMPS), and was converted to the mass concentration using the SOA density (1.3 g cm^{-3} for α-pinene SOA and 1.4 g cm^{-3} for other types of SOA) (Ng et al., 2007a; Ng et al., 2007b; Wyche et al., 2009; Xu et al., 2014). SOA were generated under varied NO$_x$ conditions (high NO$_x$ (HC/NO$_x$<10 ppbC/ppb),

10   low NO$_x$ (HC/NO$_x$>10 ppbC/ppb); Table 1). No seed aerosols were added to in this study. Other details about chamber experiments can be found in Sect. S1 of the Supporting Information. The typical time profiles of SOA mass concentration, HCs (i.e. toluene or TMB), NO$_x$, NO and O$_3$ mixing ratios through the experiments were shown in Fig. S1.

2.2 Sampling method

15   SOA and background (before chemical injection) samples were collected within a small amount of deionized (DI) water using a PILS technique. The aerosol particle that enters the PILS grows quickly into a droplet under the supersaturated environment and this droplet is collected on the plate by impaction (Orsini et al., 2003). The sampling efficiency of PILS is greater than 95 % for particle size ranging from 0.03 to 6 μm (Orsini et al., 2003). A parallel carbon filter denuder

20   (Sunset Laboratory Inc.) was placed upstream of PILS to remove gaseous compounds. The efficiency of the carbon denuder was measured by comparing the concentrations of toluene and CCl$_4$ with the carbon denuder to those without the denuder and was found to be almost 100 %. The mass concentration of SOA in the PILS sample was estimated using the chamber SOA mass concentration, the air flow rate of PILS (13 L/min), the total liquid volume collected by PILS, and

25   the collection efficiency of PILS. SOA samples collected by PILS were applied to the chemicals assays described in Sect. 2.3.

To measure the concentration of PANs in the gas phase, gaseous photooxidation products (22 Jul 2016) were collected using an impinger (filled with 5 mL DI water) at a flow rate of 0.8 L min^{-1}. A filter (13 mm diameter, Pall Life Scientific Pallflex, TX40HI20-WW) was applied upstream of

30   the impinger to remove particles. The impinger samples were then applied to PAN analysis.

2.3 Chemical assays

Detailed information about chemicals and solution preparation can be found in Sect. S2. To avoid the decay of some unstable SOA products in the aqueous solution, the analytical procedures of DTT, PAN, and organic hydroperoxides assays were completed within 24 h after sampling. Before chemical analysis, all SOA samples were stored in a refrigerator at 4 °C. The reaction schemes and quality assurance/quality control (QA/QC) details of chemicals assays are included in Sect. S3 and S4.

2.3.1 DTT assay

DTT assay was employed to quantify the oxidative potential of SOA (Cho et al., 2005; Jiang et al., 2016). In the first step (DTT oxidation), a mixture of 700 µL SOA-PILS sample, 200 µL potassium phosphate buffer (2 mM, pH=7.4) and 100 µL DTT (1 mM) was incubated at 37 °C in a sonicator (FS30H Ultrasonic Cleaner, Fisher Scientific). For the second step (determination of the remaining DTT), the reaction between DTT and SOA was quenched by adding 1 mL 1% w/v trichloroacetic acid (a commonly used quencher of thiol oxidation). Then, 0.5 mL 5,5'-dithiobis-(2-nitrobenzoic acid) solution (1 mM in methanol) was added to react with the remaining DTT forming a 2-nitro-5-thiobenzoic acid (Scheme S1), which produced a yellow color after the addition of 1 mL Tris base buffer-HNO$_3$ (pH = 8.9, 0.4 M). The absorbance of 2-nitro-5-thiobenzoic acid at 412 nm was measured using a UV/VIS Spectrometer (Lambda 35, PerkinElmer). To ensure the pseudo-1st-order reaction between DTT and redox-active species in SOA, the SOA mass applied to DTT assay was constrained to ensure that the DTT consumption remained less than 50 % of the initial DTT concentration. Background chamber air samples, blank controls (DI water) and positive controls (0.1 µM PQN) were run in duplicates for each set of measurements. The DTT loss in blank and positive controls were shown in Fig. S2 and Fig. S3. To estimate the effect of radicals produced by sonication on DTT assay, the DTT loss rate in blank control during sonication was compared to that during shaking (Edison Environmental Incubator Shaker G24, low speed, 37 °C). Tested using the statistical method based on the Student t-test (Andrade and Estévez-Pérez, 2014), the slope of DTT loss vs. time with the sonicator was not significantly different from the one with the shaker (significance level α = 0.05); therefore, in this study, the influence of free radicals generated by sonication on DTT measurement was insignificant. The blank-corrected DTT consumption (ΔDTT, nmol) was estimated by Eq. (1):

$$\Delta DTT = \frac{A_{blk} - A_{SOA}}{A_0} DTT_0 \qquad\qquad\qquad\qquad (1)$$

where A_{blk} is the absorbance of the blank control after incubation, A_{SOA} is the absorbance of the SOA sample after incubation, A_0 is the absorbance of the blank control without incubation, and DTT_0 (100 nmol) is the initial moles of DTT. Due to the instability of hydroperoxides (Fig. S4), SOA samples should be applied to chemical assays soon after collection (within 24 h).

To investigate the additivity of DTT response from different types of chemical species, ΔDTT of the blend of several compounds was compared with the sum of ΔDTT originating from individual compounds. Figure S5 proves that the DTT consumption is additive by showing that ΔDTT of the mixture of four model compounds (i.e., acrolein, PQN, H_2O_2, and tert-butyl hydroperoxides) was consistent with the sum of individuals.

2.3.2 Organic hydroperoxides analysis

The NPBA method, which had been used by Su et al. (Su et al., 2011) for the determination of H_2O_2, was extended for the quantification of alkyl and acyl hydroperoxides. NPBA reacts with organic hydroperoxides to form a 4-nitrophenol (Scheme S2), which has a large absorption coefficient at 406 nm (Kuivila, 1954; Kuivila and Armour, 1957; Su et al., 2011). A mixture of 1 mL SOA sample, 100 μL NPBA solution (10 mM in methanol), and 900 μL KOH solution (50 mM) was incubated at 85 °C. Positive control (10 μM H_2O_2) was run in duplicate for each set of measurements. The NPBA method was calibrated using aqueous 4-nitrophenol solutions ranging from 1–40 μM (Fig. S6). The feasibility of the NPBA assay was tested for peracetic acid ($CH_3C(O)OOH$), tert-butyl peroxide ($(CH_3)_3COOC(CH_3)_3$), tert-butyl hydroperoxide ($(CH_3)_3COOH$), and hydrogen peroxide (H_2O_2). Within a 90 % confidence level, the absorbance sourced from the reaction of NPBA with the known amount of organic hydroperoxides or H_2O_2 was covered by the calibration curve (Fig. S6). However, no absorbance at 406 nm appeared in the NPBA+tert-butyl peroxide mixture (data not shown). As discussed in Sect. S4.2, the multi-alcohols products and 4-nitrophenol that might be formed in SOA has no influence on the NPBA assay. For toluene SOA, the reaction of organic hydroperoxides with NPBA completed within 7 h, and for isoprene SOA within 2 h (Fig. S7). Organic hydroperoxides in aqueous solution are unstable. For example, after a 6-day storage at 4 °C, $(CH_3)_3COOH$ degraded 10 % (Fig. S8); therefore, we ensured that SOA samples were applied to chemical assays soon after collection (within 24 h).

2.3.3 PAN analysis

The concentration of PANs was quantified by Griess assay. The Griess reagent, a mixture of sulfanilic acid and n-(1-naphthyl) ethylenediamine dihydrocloride (NEDD), has been widely applied to quantify the concentration of nitrogen oxides in environmental, industrial, and

5 biological systems (Giustarini et al., 2008; Ridnour et al., 2000; Saltzman, 1954). Nitrogen oxides were transformed to nitrites that can form azo dyes when mixed with Griess reagent (Scheme S3) (Giustarini et al., 2008). For PAN analysis, a 300 µL SOA (collected by PILS) or gas sample (collected by an impinger) was mixed with 300 µL KOH aqueous solution (50 mM) for 15 min to hydrolyze PANs completely and form nitrites. As discussed in Sect. S4.3, a 15-min hydrolysis was

10 shown to be enough to hydrolyze the PANs in SOA products. Then, 1 mL Griess reagent (20 mM sulfanilic acid and 5 mM NEDD aqueous solution) was added to the mixture, and allowed to react with nitrites for 15 min. A purple-magenta color formed immediately. No difference in the absorbance was found between a 15-min reaction and a 30-min reaction. The concentration of PANs was estimated from the absorbance at 541 nm (Ridnour et al., 2000). Positive controls (10

15 µM $NaNO_2$) were run in duplicate for each set of measurements. Griess assay was calibrated using $NaNO_2$ aqueous solutions with varied concentrations (0.4–50 µM; Fig. S9).

2.3.4 DTT activity enhancement

Dou et al. (Dou et al., 2015) showed that by forming H-bonds with hydroquinones, imidazole derivatives are capable of facilitating electrons transfer from hydroquinones to molecular oxygen,

20 accelerating the redox cycling of quinones and enhancing the oxidation of DTT (Scheme S4). In the DTT enhancement test, a 250 µL 2,4-dimethylimidazole aqueous solution (5 mM) was mixed with a 450 µL SOA-PILS sample to get a 700 µL mixture. Then, 100 µL DTT solution (1 mM) and 200 µL potassium phosphate buffer (2 mM) were added to the mixture. The subsequent steps were the same as those used for the DTT assay. The enhanced DTT consumption rate ($t = 30$ min)

25 in the presence of 2,4-dimethylimidazole was measured. Positive controls (2 µM NQN) were run in duplicates for each set of measurements.

3 Results and discussion

3.1 DTT activity of SOA

The SOA yield (Y) represents a ratio of organic mass formed to HC consumed (Odum et al., 1996). As shown in Table 1, the Y values of toluene, TMB, isoprene, and α-pinene SOA ranged from 5 % to 15 %, 6 % to 8 %, 1 % to 5 %, and 14 % to 36 %, respectively. Except isoprene SOA, the SOA yields in this study were consistent with those reported in previous studies (Eddingsaas et al., 2012a; Healy et al., 2008; Odum et al., 1996; Sato et al., 2007). Our SOA yields for isoprene SOA were lower than those reported in other studies (Carlton et al., 2009; Xu et al., 2014) because the temperatures in our outdoor experiments were higher than those sourced from indoor chambers. Within the NO_x conditions (HC/NO_x=5-36 ppbC/ppb) in this study, SOA yields of high-NO_x isoprene were much higher than those of low-NO_x isoprene, and SOA yields of other three types of SOA at high NO_x conditions were generally lower than those at low NO_x conditions. Aromatic hydrocarbons (toluene and 1,3,5-trimethylbenzene) are mainly oxidized by OH radicals while biogenic hydrocarbons (isoprene or a-pinene) by both OH radicals and ozone. Based on the integrated reaction rate (IRR) analysis, the oxidation of isoprene by OH radicals is at least 3 times higher than that by ozone at the low NO_x condition (HC/NO_x=17 ppbC/ppb). The oxidation of biogenic hydrocarbons was dominated by OH radicals, particularly, in the morning.

The DTT consumption rate, DTT_t (pmol min^{-1} μg^{-1}), was defined as DTT consumption (ΔDTT, pmol) per minute of reaction time (t, min) per microgram of SOA mass (m_{SOA}, μg):

$$DTT_t = \frac{\Delta DTT}{m_{SOA} t} \tag{2}$$

Figure 2 illustrates the DTT_t (t = 30 min) of SOA produced from four different HCs under varied NO_x conditions. Overall, the influence of NO_x on DTT_t varied, depending on the type of HC. The DTT_t of toluene SOA was insensitive to NO_x for samples collected within a similar sampling period, but it decreased with increasing aging time. The DTT_t of toluene SOA reached approximately 70 pmol min^{-1} μg^{-1} by 13:00 under both high NO_x and low NO_x conditions, but decreased by about 40-50 % in the late afternoon. For aged toluene SOA, the decline of DTT_t might reflect the decay of photooxidation products that could potentially react with DTT (e.g., electron-deficient alkenes that can react with OH radicals) (Finlayson-Pitts and Pitts Jr, 2000). The lifetime of two semi-volatile electron-deficient alkenes (4-oxo-2-butenoic acid, and 2-hydroxy-3-penten-1,5-dial) that were reported in the previous study (Jang and Kamens, 2001) was estimated

using a structure-reactivity relationship for the reaction with OH radicals (typically 2×10^{-4} ppb under chamber conditions) (Finlayson-Pitts and Pitts Jr, 2000; Jang and Kamens, 2001; Kwok and Atkinson, 1995). If these two electron-deficient carbonyls are oxidized by OH radicals in the gas phase, the estimated lifetime of 4-oxo-2-butenoic acid and 2-hydroxy-3-penten-1,5-dial is

5   estimated to be 134 min and 43 min, respectively (Sect. S5). The actual lifetime of these compounds will be shorter than our estimation since they can also be oxidized in particle phase. Furthermore, some particulate oxidizers might also photochemically decompose with increasing oxidation time (Sect. 3.3). For isoprene SOA, DTT_t was significantly affected by NO_x. There was a 38 % to 69 % decrease in isoprene DTT_t when the HC/NO_x (ppbC/ppb) ratio was reduced from

10   30 to 5. Under high NO_x conditions, the DTT_t of less-aged isoprene SOA was about 50 % lower than that of less-aged toluene SOA. However, under low NO_x conditions, the DTT_t of isoprene SOA was comparable to that of toluene SOA. The DTT_t of TMB and α-pinene SOA were much lower than those of toluene and isoprene SOA, and they were not affected significantly by NO_x conditions. The DTT_t values of this study were also compared with those reported in previous

15   studies. The DTT_t values of α-pinene SOA in this study were close to those reported by Tuet et al. (Tuet et al., 2017b). The DTT_t values of isoprene SOA was, however, higher than those observed by Tuet et al. (Tuet et al., 2017b) and Kramer et al. (Kramer et al., 2016). This difference might be caused by the degree of aerosol aging under different NO_x conditions, initial OH radical sources, humidity and temperature.

20   Traditional DTT_t has been used to measure the oxidative potential originating from the catalytic redox cycling of particulate constituents (e.g., quinones and metals) (Charrier and Anastasio, 2012; Cho et al., 2005; Kumagai et al., 2002). When governed by such catalytic reactions, DTT consumption increases linearly with reaction time (Fig. S3). To demonstrate the time-dependency of DTT consumption, the reaction time of DTT assay was extended to 2 h for isoprene SOA and

25   toluene SOA, which both had high DTT_t. The mass-normalized DTT consumption (DTT_m, nmol μg^{-1}) was defined as the ratio of ΔDTT (nmol) to m_{SOA} (μg):

$$DTT_m = \frac{\Delta DTT}{m_{SOA}} \tag{3}$$

In Fig. 3, the NO_x effect on DTT_m was consistent with that on DTT_t (Fig. 2): no NO_x effect was observed on the DTT_m of toluene SOA, and the DTT_m of low-NO_x isoprene SOA was much higher

30   than that of high-NO_x isoprene SOA.

Figure 3 shows that the increase in DTT_m with time for both isoprene and toluene SOA was non-linear, suggesting that DTT consumption by SOA products was governed by non-catalytic processes. For example, DTT consumption by isoprene SOA was nearly completed within 2 h. For toluene SOA (initial HC/NO_x=6 or 18 ppbC/ppb), the increase of DTT_m also appeared to slow

5   down over a 2h reaction, although the DTT_m did not reached a plateau under the same DTT assay conditions (i.e., the same buffer concentration). Medina-Ramos et al. (Medina-Ramos et al., 2013) reported that the electron transfer rate between glutathione (GSH) and an electrogenerated mediator ($[IrCl_6]^{2-}$) exhibited a slight acceleration when the phosphate buffer concentration was increased from 0 to 50 mM at pH = 7.0. To achieve the completion of the reaction between particle

10   oxidizers in SOA and DTT, the DTT_m of toluene SOA (HC/NO_x=24 ppbC/ppb) was measured with a 0.8 mM potassium phosphate buffer in the first step of DTT assay (2 times higher than the typical buffer concentration (0.4 mM)). As shown in Fig. 3, the DTT_m of the toluene SOA (HC/NO_x=24 ppbC/ppb) reached a plateau within 2 h, proving that DTT consumption by toluene SOA was controlled by non-catalytic mechanisms. At high NO_x conditions, the DTT_m ($t = 2$ h) of

15   toluene SOA was 4–5 times higher than that of isoprene SOA. This difference was about 2 times greater than that for DTT_t (Fig. 2); therefore, we concluded that DTT_m is more suitable than DTT_t for estimating the oxidative potential of SOA, given that DTT_m can determine the maximum capacity of non-catalytic modulators in SOA to consume DTT.

3.2 DTT modulator: quinones

20   To illustrate the role of quinones in modulating the DTT responses of SOA, the enhanced DTT consumption rate ($t = 30$ min) in the presence of 2,4-dimethylimidazole was measured. The enhancement factor (pmol min^{-1} μg-SOA^{-1} μmol-imidazole^{-1}) was estimated by Eq. (4):

$$\text{Enhancement Factor} = \frac{\Delta DTT_{mix} - \Delta DTT_{SOA} - \Delta DTT_{imidazole}}{m_{SOA}\, n_{imidazole}\, t} \tag{4}$$

where $n_{imidazole}$ (μmol) is the moles of 2,4-dimethylimidazole added to the DTT reaction mixture,

25   ΔDTT_{mix} (pmol) is the DTT consumption by the mixture of SOA and 2,4-dimethylimidazole, ΔDTT_{SOA} (pmol) is the DTT consumption by SOA only, and $\Delta DTT_{imidazole}$ (pmol) is the DTT consumption by 2,4-dimethylimidazole only. As shown in Fig. 4, the enhancement factors of the four SOA were 2–3 orders of magnitude lower than those of the reference quinone compounds (i.e., NQN and PQN), suggesting that the redox cycling of quinones was not the major mechanism

30   underlying the DTT consumption by the SOA. Hamilton et al. (Hamilton et al., 2005) reported that

the total amount of identified quinones (i.e., 5-methyl-o-benzoquinone, 2-methyl-p-benzoquinone, 2-hydroxy-5-methyl-p-benzoquione) from the photooxidation of toluene was less than 0.07 % of the total aerosol mass. In a model compound study, Kumagai et al. (Kumagai et al., 2002) also reported that the oxidation of DTT by most benzoquinones (e.g., 1,4-benzoquinone, 2-methyl-p-

5 benzoquinone) was negligible under simulated physiological conditions (pH = 7.5, 37 °C).

3.3 DTT modulator: non-catalytic particulate oxidizers

In-depth investigations on the roles of non-catalytic particulate oxidizers in DTT consumption were performed for isoprene SOA and toluene SOA, which led to high DTT_t. Organic hydroperoxides and PANs can oxidize sulfhydryl groups (oxidation state of S[−2]) to disulfides

10 (S[−1]) or to even higher oxidation states (S[0], S[+2], S[+4]; Fig. 1b) (Grek et al., 2013; Mudd, 1966; Mudd and McManus, 1969). Under low NO_x conditions, alkyl peroxy radicals (RO_2) dominantly react with HO_2 radicals, producing alcohols, alkyl hydroperoxides, and carbonyls (Finlayson-Pitts and Pitts Jr, 2000; Kroll et al., 2006; Ng et al., 2007b). Under high NO_x conditions, RO_2 radicals mainly react with NO generating aldehydes (Finlayson-Pitts and Pitts Jr, 2000). The

15 reaction of aldehydes with OH radicals followed by the reaction with molecular oxygen yields peroxy acyl radicals (RC(O)OO) (Finlayson-Pitts and Pitts Jr, 2000). RC(O)OO can react with NO_2 to form PANs and react with HO_2 radicals to form RC(O)OOH (Finlayson-Pitts and Pitts Jr, 2000; Nguyen et al., 2012; Xu et al., 2014). In this study, the nanomoles of organic hydroperoxides per microgram of SOA were quantified using the NPBA assay, represented by $[OHP]_m$ (nmol μg-

20 SOA^{-1}). The nanomoles of PANs per microgram of SOA was measured by the Griess assay, represented by $[PAN]_m$ (nmol μg-SOA^{-1}).

As shown in Fig. 5a, by increasing the HC/NO_x (ppbC/ppb) from 5 to 27, $[OHP]_m$ in isoprene SOA increased 2 times owing to the organic hydroperoxides formed from the RO_2+HO_2 reaction pathway under low NO_x conditions. Under the experimental conditions of this study, the influence

25 of NO_x on $[OHP]_m$ in toluene SOA was insignificant. Presumably, the aging process reduced the significance of the NO_x effect on $[OHP]_m$. Low-NO_x toluene SOA was collected about 2 h later (i.e., a greater degree of aging) than high-NO_x toluene SOA. The organic hydroperoxides in the low-NO_x toluene experiment degraded more through photolysis or photooxidation (Lee et al., 2000) than those in the high-NO_x toluene experiment. The effect of the aging process on toluene

30 $[OHP]_m$ was consistent with that on toluene DTT_t (Fig. 2).

As shown in Fig. 5b, $[PAN]_m$ was found to be one order of magnitude lower than $[OHP]_m$. With the decrease in HC/NO_x (ppbC/ppb) from about 22 to 9, $[PAN]_m$ in the toluene SOA increased 3 times as a result of PANs production from the RO_2+NO reaction pathway under high NO_x conditions (Fig. 1a) (Xu et al., 2014). For isoprene, the moles of both aerosol phase PANs and gas phase PANs per cubic of air volume were significantly greater at higher NO_x levels (Fig. S10). Most PAN products from the photooxidation of isoprene existed in the gas phase and the amount of PAN in particle phase was trivial (Fig. S10); for example, aerosol phase PAN products was only 0.5 % of gas phase PAN products.

To underline the contribution of organic hydroperoxides and PANs to the DTT_m of SOA, the DTT_m values of toluene and isoprene SOA were also compared with the sum of $[OHP]_m$ and $[PAN]_m$. Figure 5c shows that organic hydroperoxides were the major products that induced the oxidative potential of isoprene SOA. For toluene SOA, only 45–65 % of DTT_m could be ascribed to organic hydroperoxides, and the remaining fraction was attributed to other organic compounds in SOA. We propose that electron-deficient alkenes, abundant in toluene SOA (Jang and Kamens, 2001), can substantially modify sulfhydryl groups in DTT via a Michael addition (Fig. 1b) (Nair et al., 2014). In the next section, the reactivity of electron-deficient alkenes with DTT will be demonstrated using selected model compounds.

3.4 DTT modulator: electron-deficient alkenes

Figure 6 illustrates the DTT_t (t = 30 min) of four electron-deficient alkenes (i.e., acrolein, methacrolein, 2,4-hexadienal, and mesityl oxide). Acrolein showed much higher DTT_t than the other compounds. The susceptibility of an alkene to a Michael addition reaction depends on the nature of the electron withdrawing group coupled to the C=C bond (Nair et al., 2014). The methyl group of methacrolein and mesityl oxide is an electron donating group that increases the electron density on the C=C bond; thus, decreasing the reactivity of the C=C bond with DTT. The extended conjugation (C=C-C=C-C(O)H) in 2,4-hexadienal stabilizes the C=C bond leading to an extremely low DTT_t.

The alkenes from the photooxidation of toluene were usually coupled with electron withdrawing groups such as carbonyls, nitrates, and carboxylic acids (Jang and Kamens, 2001). These electron-withdrawing groups enable the alkenes to be reactive with DTT. Compared with toluene SOA, TMB SOA will have more alkyl substituted alkenes owing to the three methyl groups on the

aromatic ring, and therefore be less reactive with DTT. This tendency partially explains why the DTT_t of TMB SOA was significantly lower than that of toluene SOA (Fig. 2). Based on aerosol composition predictions using predictive SOA models such as the Unified Partitioning Aerosol Phase Reaction (UNIPAR) model, the mass fraction of electron-deficient alkenes in high-NO_x

5   toluene SOA should be more than 50 % (Im et al., 2014); therefore, the gap between toluene DTT_m and concentrations of non-catalytic particulate oxidizers (Fig. 5c) might be filled by abundant electron-deficient alkenes.

4 Atmospheric implications and conclusions

The influence of NO_x on the oxidative potential of SOA was investigated using DTT_t (Fig. 2).

10   Among four HCs, only isoprene SOA was significantly sensitive to NO_x levels, showing much higher DTT_t at lower NO_x conditions. The DTT_t of toluene SOA was found to be lower with a longer aging time, regardless of NO_x conditions.

For SOA consisting of non-catalytic redox compounds, DTT_m is more appropriate than DTT_t for assessing oxidative potential, because of the non-linear relationship between DTT consumption

15   and reaction time (Fig. 3). A decrease in isoprene DTT_m was observed with increasing NO_x levels, but no significant NO_x effect on DTT_m was observed for toluene SOA within a 2h reaction. To apply the DTT_m results of this study to ambient atmosphere, DTT_m should be coupled with SOA mass concentrations. Under high NO_x conditions, the DTT_m of toluene SOA was almost 5 times higher than that of isoprene SOA, underlining the importance of toluene in urban areas, despite of

20   its lower SOA yield (Table 1) in the urban environment (i.e., higher NO_x conditions). In spite of relatively low DTT_m for high-NO_x isoprene SOA, isoprene could still play a substantial role in the oxidative potential of ambient urban aerosols, because of its abundance (Guenther et al., 2006) and high SOA yields (Table 1) under high NO_x conditions. The NO_x effect on the DTT_m of isoprene SOA is limited to the NO_x conditions applied in this study, and should be extended to a variety of

25   HC/NO_x ratios in further studies.

As discussed in Sect. 3.1 and 3.2, the DTT consumption by SOA was not sourced from quinones, which can catalytically yield ROS. Hence, the contribution of non-catalytic particulate oxidizers, especially organic hydroperoxides, to the oxidative potential of SOA was highlighted in this study. Non-catalytic particulate oxidizers account for almost 100 % of isoprene DTT_m, and 45–65 % of

toluene DTT_m (Fig. 5c).   In addition to non-catalytic particulate oxidizers, electron-deficient alkenes in toluene SOA can potentially react with DTT via a Michael addition (Nair et al., 2014). The results of this study also show that some of the oxidizers (e.g., PANs) formed from the photooxidation of hydrocarbons predominantly exist in the gas phase (Fig. S10).   Future studies should further consider how, through absorption into the bio-system, gas phase oxidizers may be effectual for inducing oxidative stress.

Supplement. The Supplement related to this article is available.

Competing interests. The authors declare that they have no conflict of interest.

Acknowledgement. This work was supported by a grant (2014M3C8A5032316) from the Ministry of Science, ICT, and Future Planning at South Korea.

References

Andrade, J. M. and Estévez-Pérez, M. G.: Statistical comparison of the slopes of two regression lines: A tutorial, Analytica Chimica Acta, 838, 1-12, 2014.

Antiñolo, M., Willis, M. D., Zhou, S., and Abbatt, J. P.: Connecting the oxidation of soot to its redox cycling abilities, Nat. Commun., 6, 6812, 2015.

Brook, R. D., Rajagopalan, S., Pope, C. A., Brook, J. R., Bhatnagar, A., Diez-Roux, A. V., Holguin, F., Hong, Y., Luepker, R. V., Mittleman, M. A., Peters, A., Siscovick, D., Smith, S. C., Whitsel, L., and Kaufman, J. D.: Particulate matter air pollution and cardiovascular disease, AHA Scientific Statement, 121, 2331-2378, 2010.

Carlton, A., Wiedinmyer, C., and Kroll, J.: A review of Secondary Organic Aerosol (SOA) formation from isoprene, Atmospheric Chemistry and Physics, 9, 4987-5005, 2009.

Charrier, J. and Anastasio, C.: On dithiothreitol (DTT) as a measure of oxidative potential for ambient particles: evidence for the importance of soluble transition metals, Atmos. Chem. Phys., 12, 9321-9333, 2012.

Chen, Y., Ebenstein, A., Greenstone, M., and Li, H.: Evidence on the impact of sustained exposure to air pollution on life expectancy from China's Huai River policy, P. Natl. A. Sci., 110, 12936-12941, 2013.

Cho, A. K., Sioutas, C., Miguel, A. H., Kumagai, Y., Schmitz, D. A., Singh, M., Eiguren-Fernandez, A., and Froines, J. R.: Redox activity of airborne particulate matter at different sites in the Los Angeles Basin, Environ. Res., 99, 40-47, 2005.

Chung, M. Y., Lazaro, R. A., Lim, D., Jackson, J., Lyon, J., Rendulic, D., and Hasson, A. S.: Aerosol-borne quinones and reactive oxygen species generation by particulate matter extracts, Environ. Sci. Technol., 40, 4880-4886, 2006.

Danielsen, P. H., Møller, P., Jensen, K. A., Sharma, A. K., Wallin, H., Bossi, R., Autrup, H., Mølhave, L., Ravanat, J.-L., Briedé, J. J., de Kok, T. M., and Loft, S.: Oxidative stress, DNA damage, and inflammation induced by ambient air and wood smoke particulate matter in human A549 and THP-1 cell lines, Chem. Res. Toxicol., 24, 168-184, 2011.

Davidson, C. I., Phalen, R. F., and Solomon, P. A.: Airborne particulate matter and human health: a review, Aerosol. Sci. Tech., 39, 737-749, 2005.

Docherty, K. S., Wu, W., Lim, Y. B., and Ziemann, P. J.: Contributions of organic peroxides to secondary aerosol formed from reactions of monoterpenes with O3, Environ. Sci. Technol., 39, 4049-4059, 2005.

Dou, J., Lin, P., Kuang, B.-Y., and Yu, J. Z.: Reactive oxygen species production mediated by humic-like substances in atmospheric aerosols: enhancement effects by pyridine, imidazole, and their derivatives, Environ. Sci. Technol., 49, 6457-6465, 2015.

Eddingsaas, N., Loza, C., Yee, L., Chan, M., Schilling, K., Chhabra, P., Seinfeld, J., and Wennberg, P.: α-pinene photooxidation under controlled chemical conditions–Part 2: SOA yield and composition in low-and high-NOx environments, Atmos. Chem. Phys, 12, 7413-7427, 2012a.

Eddingsaas, N. C., Loza, C. L., Yee, L. D., Seinfeld, J. H., and Wennberg, P. O.: α-pinene photooxidation under controlled chemical conditions – Part 1: Gas-phase composition in low- and high-NOx environments, Atmos. Chem. Phys., 12, 6489-6504, 2012b.

Finlayson-Pitts, B. J. and Pitts Jr, J. N.: Chapter 6 - Rates and mechanisms of gas-phase reactions in irradiated organic −NOx—air mixtures. In: Chemistry of the Upper and Lower Atmosphere, Pitts, B. J. F.-P. N. (Ed.), Academic Press, San Diego, 2000.

Forstner, H. J. L., Flagan, R. C., and Seinfeld, J. H.: Secondary organic aerosol from the photooxidation of aromatic hydrocarbons: molecular composition, Environ. Sci. Technol., 31, 1345-1358, 1997.

Fujitani, Y., Sato, K., Furuyama, A., Fushimi, A., Ito, T., Tanabe, K., Hirano, S., Imamura, T., and Takami, A.: Generation of secondary organic aerosols in a small chamber for toxicity studies, Earozoru Kenkyu, 27, 350-356, 2012.

Gelencsér, A., May, B., Simpson, D., Sánchez-Ochoa, A., Kasper-Giebl, A., Puxbaum, H., Caseiro, A., Pio, C., and Legrand, M.: Source apportionment of PM2.5 organic aerosol over Europe: Primary/secondary, natural/anthropogenic, and fossil/biogenic origin, J. Geophys. Res.-Atmos., 112, 2007.

Giustarini, D., Rossi, R., Milzani, A., and Dalle-Donne, I.: Nitrite and nitrate measurement by Griess reagent in human plasma: evaluation of interferences and standardization, Method. Enzymol., 440, 361-380, 2008.

Grek, C. L., Zhang, J., Manevich, Y., Townsend, D. M., and Tew, K. D.: Causes and consequences of cysteine S-glutathionylation, J. Bio. Chem., 288, 26497-26504, 2013.

Guenther, A., Karl, T., Harley, P., Wiedinmyer, C., Palmer, P. I., and Geron, C.: Estimates of global terrestrial isoprene emissions using MEGAN (Model of Emissions of Gases and Aerosols from Nature), Atmos. Chem. Phys., 6, 3181-3210, 2006.

Hallquist, M., Wenger, J., Baltensperger, U., Rudich, Y., Simpson, D., Claeys, M., Dommen, J., Donahue, N., George, C., and Goldstein, A.: The formation, properties and impact of secondary organic aerosol: current and emerging issues, Atmos. Chem. Phys., 9, 5155-5236, 2009.

Hamilton, J. F., Webb, P. J., Lewis, A. C., and Reviejo, M. M.: Quantifying small molecules in secondary organic aerosol formed during the photo-oxidation of toluene with hydroxyl radicals, Atmos. Environ., 39, 7263-7275, 2005.

Healy, R., Wenger, J., Metzger, A., Duplissy, J., Kalberer, M., and Dommen, J.: Gas/particle partitioning of carbonyls in the photooxidation of isoprene and 1, 3, 5-trimethylbenzene, Atmospheric Chemistry and Physics, 8, 3215-3230, 2008.

Hedayat, F., Stevanovic, S., Miljevic, B., Bottle, S., and Ristovski, Z.: Review-evaluating the molecular assays for measuring the oxidative potential of particulate matter, Chem. Ind. Chem. Eng. Q., 21, 201-210, 2014.

Im, Y., Jang, M., and Beardsley, R. L.: Simulation of aromatic SOA formation using the lumping model integrated with explicit gas-phase kinetic mechanisms and aerosol-phase reactions, Atmos. Chem. Phys., 14, 4013-4027, 2014.

Jakober, C. A., Riddle, S. G., Robert, M. A., Destaillats, H., Charles, M. J., Green, P. G., and Kleeman, M. J.: Quinone emissions from gasoline and diesel motor vehicles, Environ. Sci. Technol., 41, 4548-4554, 2007.

Jang, M., Ghio, A. J., and Cao, G.: Exposure of BEAS-2B cells to secondary organic aerosol coated on magnetic nanoparticles, Chem. Res. Toxicol., 19, 1044-1050, 2006.

Jang, M. and Kamens, R. M.: Characterization of secondary aerosol from the photooxidation of toluene in the presence of NOx and 1-propene, Environ. Sci. Technol., 35, 3626-3639, 2001.

Jansen, K. L., Larson, T. V., Koenig, J. Q., Mar, T. F., Fields, C., Stewart, J., and Lippmann, M.: Associations between health effects and particulate matter and black carbon in subjects with respiratory disease, Environ. Health Persp., 113, 1741-1746, 2005.

Janssen, N. A. H., Yang, A., Strak, M., Steenhof, M., Hellack, B., Gerlofs-Nijland, M. E., Kuhlbusch, T., Kelly, F., Harrison, R., Brunekreef, B., Hoek, G., and Cassee, F.: Oxidative potential of particulate matter collected at sites with different source characteristics, Sci. Total Environ., 472, 572-581, 2014.

Jiang, H., Jang, M., Sabo-Attwood, T., and Robinson, S. E.: Oxidative potential of secondary organic aerosols produced from photooxidation of different hydrocarbons using outdoor chamber under ambient sunlight, Atmos. Environ., 131, 382-389, 2016.

Kanakidou, M., Seinfeld, J. H., Pandis, S. N., Barnes, I., Dentener, F. J., Facchini, M. C., Van Dingenen, R., Ervens, B., Nenes, A., Nielsen, C. J., Swietlicki, E., Putaud, J. P., Balkanski, Y., Fuzzi, S., Horth, J., Moortgat, G. K., Winterhalter, R., Myhre, C. E. L., Tsigaridis, K., Vignati, E., Stephanou, E. G., and Wilson, J.: Organic aerosol and global climate modelling: a review, Atmos. Chem. Phys., 5, 1053-1123, 2005.

Katsouyanni, K., Touloumi, G., Spix, C., Schwartz, J., Balducci, F., Medina, S., Rossi, G., Wojtyniak, B., Sunyer, J., Bacharova, L., Schouten, J. P., Ponka, A., and Anderson, H. R.: Short term effects of ambient sulphur dioxide and particulate matter on mortality in 12 European cities: results from time series data from the APHEA project, BMJ, 314, 1658, 1997.

Kramer, A. J., Rattanavaraha, W., Zhang, Z., Gold, A., Surratt, J. D., and Lin, Y.-H.: Assessing the oxidative potential of isoprene-derived epoxides and secondary organic aerosol, Atmos. Environ., 130, 211-218, 2016.

Kroll, J. H., Ng, N. L., Murphy, S. M., Flagan, R. C., and Seinfeld, J. H.: Secondary organic aerosol formation from isoprene photooxidation, Environ. Sci. Technol., 40, 1869-1877, 2006.

Kuivila, H. G.: Electrophilic displacement reactions. III. kinetics of the reaction between hydrogen peroxide and benzeneboronic acid1, J. Am. Chem. Soc., 76, 870-874, 1954.

Kuivila, H. G. and Armour, A. G.: Electrophilic displacement reactions. IX. effects of substituents on rates of reactions between hydrogen peroxide and benzeneboronic acid1-3, J. Am. Chem. Soc., 79, 5659-5662, 1957.

Kumagai, Y., Koide, S., Taguchi, K., Endo, A., Nakai, Y., Yoshikawa, T., and Shimojo, N.: Oxidation of proximal protein sulfhydryls by phenanthraquinone, a component of diesel exhaust particles, Chem. Res. Toxicol., 15, 483-489, 2002.

Kumagai, Y., Shinkai, Y., Miura, T., and Cho, A. K.: The chemical biology of naphthoquinones and its environmental implications, Annu. Rev. Pharmacol., 52, 221-247, 2012.

Kwok, E. S. C. and Atkinson, R.: Estimation of hydroxyl radical reaction rate constants for gas-phase organic compounds using a structure-reactivity relationship: An update, Atmospheric Environment, 29, 1685-1695, 1995.

Lee, M., Heikes, B. G., and O'Sullivan, D. W.: Hydrogen peroxide and organic hydroperoxide in the troposphere: a review, Atmos. Environ., 34, 3475-3494, 2000.

Li, N., Sioutas, C., Cho, A., Schmitz, D., Misra, C., Sempf, J., Wang, M., Oberley, T., Froines, J., and Nel, A.: Ultrafine particulate pollutants induce oxidative stress and mitochondrial damage, Environ. Health Persp., 111, 455-460, 2003.

Li, N., Xia, T., and Nel, A. E.: The role of oxidative stress in ambient particulate matter-induced lung diseases and its implications in the toxicity of engineered nanoparticles, Free Radical Bio. Med., 44, 1689-1699, 2008.

Lin, Y.-H., Arashiro, M., Martin, E., Chen, Y., Zhang, Z., Sexton, K. G., Gold, A., Jaspers, I., Fry, R. C., and Surratt, J. D.: Isoprene-derived secondary organic aerosol induces the expression of oxidative stress response genes in human lung cells, Environ. Sci. Technol. Lett., 3, 250-254, 2016.

McDonald, J. D., Doyle-Eisele, M., Campen, M. J., Seagrave, J., Holmes, T., Lund, A., Surratt, J. D., Seinfeld, J. H., Rohr, A. C., and Knipping, E. M.: Cardiopulmonary response to inhalation of biogenic secondary organic aerosol, Inhal. Toxicol., 22, 253-265, 2010.

McWhinney, R. D., Zhou, S., and Abbatt, J. P. D.: Naphthalene SOA: redox activity and naphthoquinone gas–particle partitioning, Atmos. Chem. Phys., 13, 9731-9744, 2013.

Medina-Ramos, J., Oyesanya, O., and Alvarez, J. C.: Buffer effects in the kinetics of concerted proton-coupled electron transfer: the electrochemical oxidation of glutathione mediated by [IrCl6]2–at variable buffer pKa and concentration, J. Phys. Chem. C, 117, 902-912, 2013.

Mudd, J. B.: Reaction of peroxyacetyl nitrate with glutathione, J. Bio. Chem., 241, 4077-4080, 1966.

Mudd, J. B. and McManus, T. T.: Products of the reaction of peroxyacetyl nitrate with sulfhydryl compounds, Archives of Biochemistry and Biophysics, 132, 237-241, 1969.

Nair, D. P., Podgórski, M., Chatani, S., Gong, T., Xi, W., Fenoli, C. R., and Bowman, C. N.: The thiol-michael addition click reaction: a powerful and widely used tool in materials chemistry, Chem. Mater., 26, 724-744, 2014.

Nel, A.: Air pollution-related illness: effects of particles, Science, 308, 804-806, 2005.

Ng, N., Chhabra, P., Chan, A., Surratt, J., Kroll, J., Kwan, A., McCabe, D., Wennberg, P., Sorooshian, A., and Murphy, S.: Effect of NOx level on secondary organic aerosol (SOA) formation from the photooxidation of terpenes, Atmos. Chem. Phys., 7, 5159-5174, 2007a.

Ng, N., Kroll, J., Chan, A., Chhabra, P., Flagan, R., and Seinfeld, J.: Secondary organic aerosol formation from m-xylene, toluene, and benzene, Atmos. Chem. Phys., 7, 3909-3922, 2007b.

Nguyen, T. B., Laskin, A., Laskin, J., and Nizkorodov, S. A.: Direct aqueous photochemistry of isoprene high-NOx secondary organic aerosol, Phys. Chem. Chem. Phys., 14, 9702-9714, 2012.

Odum, J. R., Hoffmann, T., Bowman, F., Collins, D., Flagan, R. C., and Seinfeld, J. H.: Gas/particle partitioning and secondary organic aerosol yields, Environ. Sci. Technol., 30, 2580-2585, 1996.

Orsini, D. A., Ma, Y., Sullivan, A., Sierau, B., Baumann, K., and Weber, R. J.: Refinements to the particle-into-liquid sampler (PILS) for ground and airborne measurements of water soluble aerosol composition, Atmos. Environ., 37, 1243-1259, 2003.

Pindado Jiménez, O., Pérez Pastor, R. M., Vivanco, M. G., and Santiago Aladro, M.: A chromatographic method to analyze products from photo-oxidation of anthropogenic and biogenic mixtures of volatile organic compounds in smog chambers, Talanta, 106, 20-28, 2013.

Ridnour, L. A., Sim, J. E., Hayward, M. A., Wink, D. A., Martin, S. M., Buettner, G. R., and Spitz, D. R.: A spectrophotometric method for the direct detection and quantitation of nitric oxide, nitrite, and nitrate in cell culture media, Anal. Biochem., 281, 223-229, 2000.

Saltzman, B. E.: Colorimetric microdetermination of nitrogen dioxide in atmosphere, Anal. Chem., 26, 1949-1955, 1954.

Sato, K., Hatakeyama, S., and Imamura, T.: Secondary Organic Aerosol Formation during the Photooxidation of Toluene: NOx Dependence of Chemical Composition, The Journal of Physical Chemistry A, 111, 9796-9808, 2007.

Sato, K., Takami, A., Kato, Y., Seta, T., Fujitani, Y., Hikida, T., Shimono, A., and Imamura, T.: AMS and LC/MS analyses of SOA from the photooxidation of benzene and 1,3,5-trimethylbenzene in the presence of NOx: effects of chemical structure on SOA aging, Atmos. Chem. Phys., 12, 4667-4682, 2012.

Saunders, S. M., Jenkin, M. E., Derwent, R. G., and Pilling, M. J.: Protocol for the development of the Master Chemical Mechanism, MCM v3 (Part A): tropospheric degradation of non-aromatic volatile organic compounds, Atmos. Chem. Phys., 3, 161-180, 2003.

Saunders, S. M., Jenkin, M. E., Derwent, R. G., and Pilling, M. J.: World wide web site of a master chemical mechanism (MCM) for use in tropospheric chemistry models, Atmos. Environ., 31, 1249, 1997.

Shiraiwa, M., Yee, L. D., Schilling, K. A., Loza, C. L., Craven, J. S., Zuend, A., Ziemann, P. J., and Seinfeld, J. H.: Size distribution dynamics reveal particle-phase chemistry in organic aerosol formation, P. Natl. A. Sci., 110, 11746-11750, 2013.

Su, G., Wei, Y., and Guo, M.: Direct colorimetric detection of hydrogen peroxide using 4-nitrophenyl boronic acid or its pinacol ester, Am. J. Analyt. Chem., 2, 879-884, 2011.

Tuet, W. Y., Chen, Y., Fok, S., Champion, J. A., and Ng, N. L.: Inflammatory responses to secondary organic aerosols (SOA) generated from biogenic and anthropogenic precursors, Atmos. Chem. Phys. Discuss., 2017, 1-42, 2017a.

Tuet, W. Y., Chen, Y., Xu, L., Fok, S., Gao, D., Weber, R. J., and Ng, N. L.: Chemical oxidative potential of secondary organic aerosol (SOA) generated from the photooxidation of biogenic and anthropogenic volatile organic compounds, Atmos. Chem. Phys., 17, 839-853, 2017b.

van Eeden, S. F., Yeung, A., Quinlam, K., and Hogg, J. C.: Systemic Response to Ambient Particulate Matter, Proc. Am. Thorac. Soc., 2, 61-67, 2005.

Verma, V., Fang, T., Xu, L., Peltier, R. E., Russell, A. G., Ng, N. L., and Weber, R. J.: Organic aerosols associated with the generation of reactive oxygen species (ROS) by water-soluble PM2.5, Environ. Sci. Technol., 49, 4646-4656, 2015.

Wyche, K. P., Monks, P. S., Ellis, A. M., Cordell, R. L., Parker, A. E., Whyte, C., Metzger, A., Dommen, J., Duplissy, J., Prevot, A. S. H., Baltensperger, U., Rickard, A. R., and Wulfert, F.: Gas phase precursors to anthropogenic secondary organic aerosol: detailed observations of 1,3,5-trimethylbenzene photooxidation, Atmos. Chem. Phys., 9, 635-665, 2009.

Xu, L., Kollman, M. S., Song, C., Shilling, J. E., and Ng, N. L.: Effects of NOx on the volatility of secondary organic aerosol from isoprene photooxidation, Environ. Sci. Technol., 48, 2253-2262, 2014.

Zheng, W., Flocke, F. M., Tyndall, G. S., Swanson, A., Orlando, J. J., Roberts, J. M., Huey, L. G., and Tanner, D. J.: Characterization of a thermal decomposition chemical ionization mass

spectrometer for the measurement of peroxy acyl nitrates (PANs) in the atmosphere, Atmos. Chem. Phys., 11, 6529-6547, 2011.

Table 1. Outdoor chamber experiment conditions

HC and Date	Initial HC ppb	Initial NO$_x$ (HONO) [a] ppb	Initial HC/NO$_x$ ppbC/ppb	[SOA]$_{max}$ [b] μg/m^3	ΔHC [c] ppb	Y %	Mid-collection time [d]	RH [e] %	Temp [e] K	Chemical assay [f]
Toluene										
13 Feb 2016	641	525 (193)	9	229	403	15.1	13:40	22–63	281–303	DTT
01 May 2016	935	766 (133)	9	348	631	14.6	14:20	18–46	294–316	DTT, PAN
01 May 2016	938	301 (73)	22	292	542	14.3	12:10	21–48	294–315	DTT, PAN
23 May 2016	691	906 (250)	5	148	546	7.1	13:20	18–60	288–315	DTT, Enhance
23 May 2016	735	313 (86)	16	147	421	9.3	15:40	15–22	307–316	DTT, Enhance
18 Aug 2016	640	783 (179)	6	178	517	9.1	12:30	24–61	297–319	DTT, OHP
06 Aug 2016	610	240 (55)	18	75	216	9.2	12:30	43–59	297–305	DTT
18 Aug 2016	342	107 (24)	22	44	227	5.2	14:20	20–38	303–321	OHP
17 Nov 2016	622	179 (43)	24	139	452	8.1	13:20	12–56	282–309	DTT [g]
TMB										
04 Oct 2015	613	920	6	201	613	6.7	14:40	20–43	290–310	DTT
04 Oct 2015	657	310	19	207	542	7.8	13:20	24–46	290–306	DTT
20 Feb 2016	589	1024	5	150	548	5.6	13:00	14–60	282–311	DTT
20 Feb 2016	583	156	34	128	455	5.7	14:40	16–61	282–311	DTT
11 Jan 2016	595	256	21	114	414	5.6	15:50	23–81	274–298	Enhance
Isoprene										
23 Apr 2016	2693	2680	5	352	2693	4.7	12:00	18–48	290–314	DTT
23 Apr 2016	2755	430	32	93	2755	1.2	13:30	23–51	290–312	DTT
14 May 2016	2928	2800	5	406	2928	5.0	14:20	17–47	292–315	DTT, Enhance
14 May 2016	2858	423	34	107	2858	1.3	12:00	25–55	293–312	DTT
22 Jul 2016	2525	2423	5	246	2525	3.5	13:20	20–55	297–320	PAN (gas) [h]
22 Jul 2016	2718	473	29	70	2718	0.9	12:50	23–58	297–320	PAN (gas) [h]
20 Aug 2016	3060	3300	5	279	3060	3.3	12:30	20–58	296–321	DTT, OHP, PAN
20 Aug 2016	3173	583	27	125	3173	1.4	11:50	25–61	297–318	DTT, OHP, PAN
α-Pinene										
25 Feb 2016	319	639	5	257	319	14.5	15:00	21–63	278–299	DTT
25 Feb 2016	323	91	36	650	323	36.1	13:30	25–67	278–298	DTT
18 Jan 2016	257	144	18	223	257	15.6	15:50	25–78	275–297	Enhance

[a] For toluene experiments, NO$_x$ was contributed by NO, NO$_2$ and HONO. The concentration of HONO was estimated using the difference in the NO$_2$ signal with and without the base denuder (1 % Na$_2$CO$_3$+1 % glucose).
[b] [SOA]$_{max}$ is the maximum SOA concentration during the aerosol collection.
[c] ΔHC is the consumption of HC when the SOA concentration reached to a maximum during the aerosol collection.
[d] This column is the mid-collection time (based on the Eastern Standard Time (EST)) of SOA sampling.
[e] The RH and temperature conditions shown in the Table 1 were recorded from the beginning of photooxidation (sunrise) until the ending of PILS sampling.
[f] The SOA samples were applied to a series of chemical assays, namely DTT assay (DTT), DTT enhancement (Enhance), organic hydroperoxides analysis (OHP), and PAN analysis (PAN).
[g] For DTT measurement of toluene SOA sample collected on 17 Nov. 2016, the concentration of potassium phosphate buffer (0.8 mM) in the first step of DTT assay was two times higher than the typical buffer concentration (0.4 mM). The DTT$_m$ of the toluene SOA sample (17 Nov. 2016) is shown in Fig. 3.
[h] The concentration of gaseous PAN products (collected by an impinger) was measured by the Griess assay.
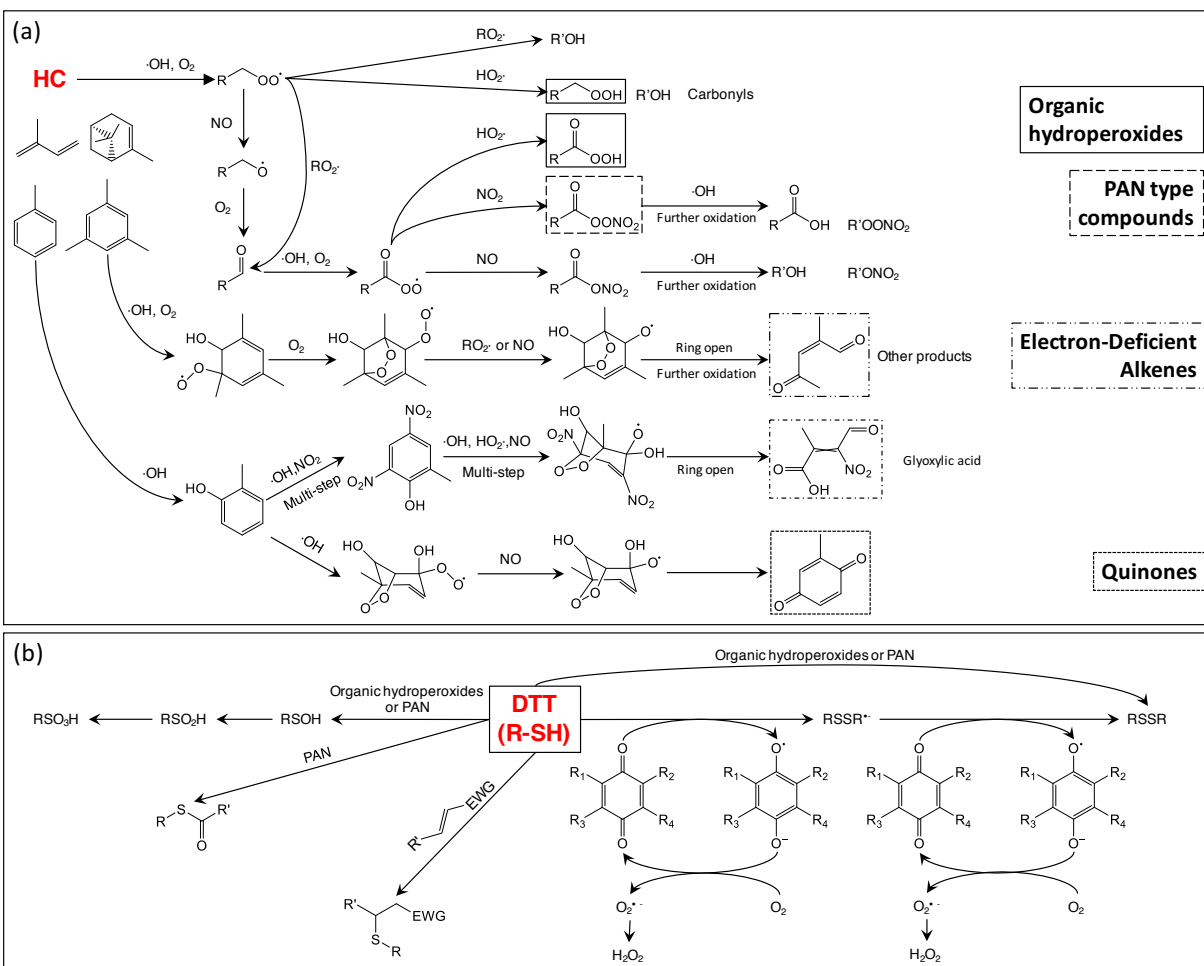
Figure 1. (a) Simplified mechanisms for the formation of alkyl and acyl hydroperoxides, peroxy acyl nitrates (PANs), electron-deficient alkenes, and quinones (Eddingsaas et al., 2012b; Jang and Kamens, 2001; Saunders et al., 2003, 1997; Wyche et al., 2009; Xu et al., 2014). Photooxidation products are not limited to the compounds shown. (b) Possible reaction mechanisms between sulfhydryl groups in dithiothreitol (DTT, represented by R-SH) and SOA products (Grek et al., 2013; Kumagai et al., 2002; Mudd, 1966; Mudd and McManus, 1969; Nair et al., 2014). EWG represents the electron-withdrawing group attached to an alkene.
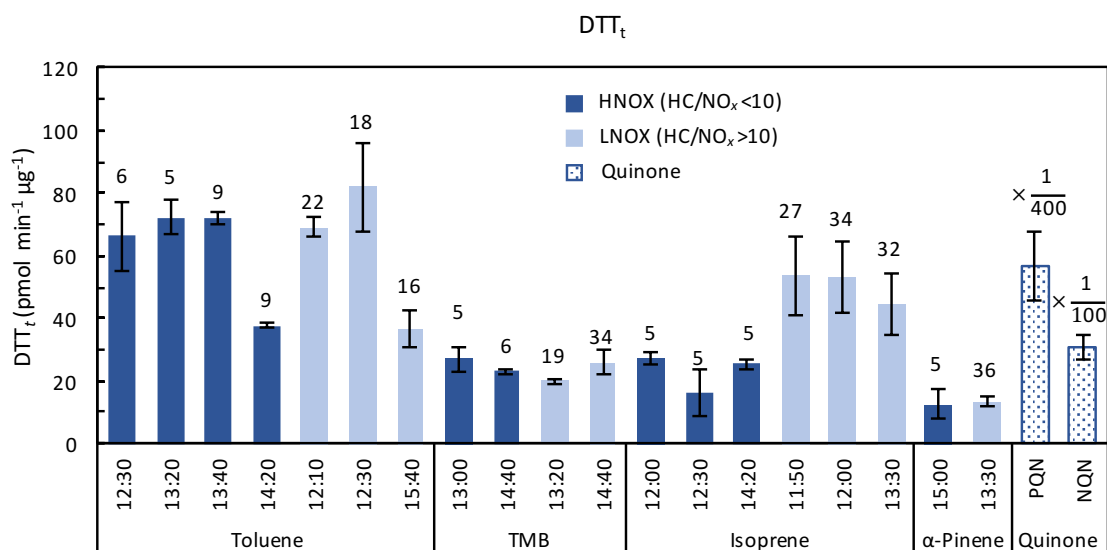
Figure 2. DTT$_t$ of chamber-generated SOA under varied NO$_x$ conditions (HNOX: high NO$_x$, LNOX: low NO$_x$) and positive controls (i.e., PQN and NQN). The number above each column represents the initial HC/NO$_x$ ratio. The x-axis represents the mid-collection time (Table 1). The DTT$_t$ of PQN and NQN are divided by 400 and 100, respectively. Each error bar was calculated by $t_{0.95} \times \sigma/\sqrt{n}$, where $t_{0.95}$ is the t-score (4.303 for n = 3 replicates) with a two-tail 95 % confidence level.

DTT$_m$ of SOA
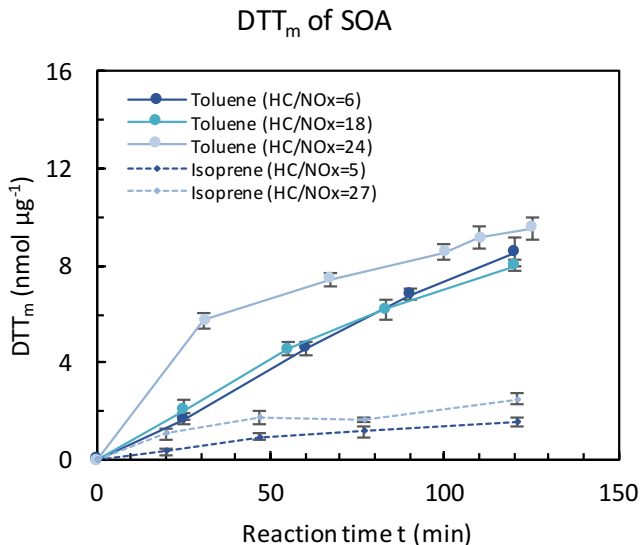
Figure 3. The time profile of DTT$_m$ for toluene and isoprene SOA under different NO$_x$ conditions. To achieve the completion of the reaction between DTT and SOA, the DTT$_m$ of toluene sample (initial HC/NO$_x$=24 ppbC/ppb collected on 17 Nov. 2016) was measured with a 0.8 mM potassium phosphate buffer in the first step of DTT assay (2 times higher than the typical buffer concentration (0.4 mM)). Each error bar was calculated by $t_{0.95} \times \sigma / \sqrt{n}$ using three replicates, where $t_{0.95}$ is the t-score (4.303 for n = 3 replicates) with a two-tail 95 % confidence level.
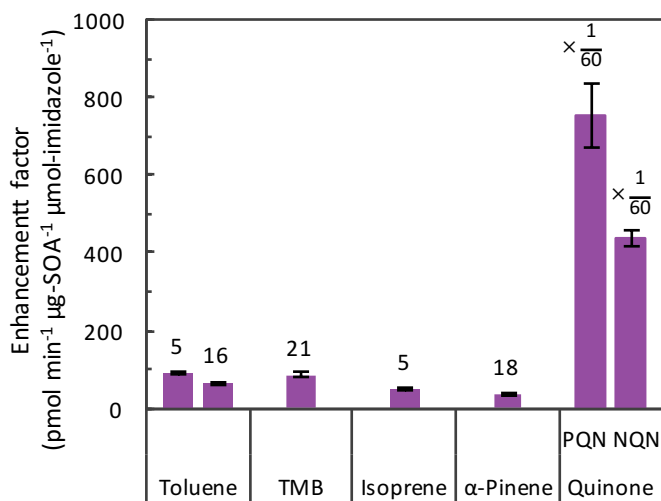
Figure 4. Enhancement factors (pmol min^{-1} µg-SOA^{-1} µmol-imidazole^{-1}) of SOA in the presence of 2,4-dimethylimidazole. The label above each column represents the initial HC/NO$_x$ ratio. The enhancement factor is expressed as the mean (± σ) of three replicates. The enhancement factors of PQN and NQN are divided by 60.
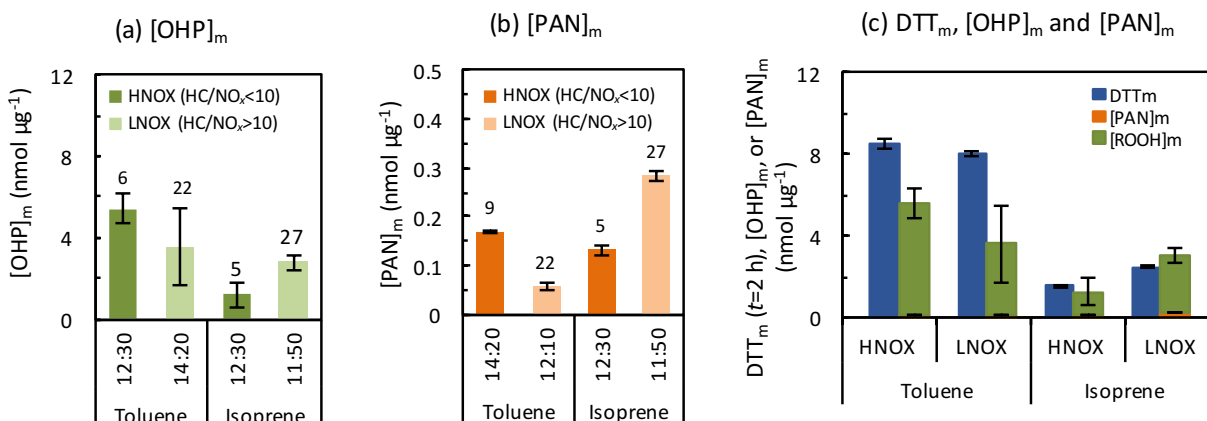
Figure 5. (a) Concentration of organic hydroperoxides in SOA, [OHP]$_m$ (nmol μg^{-1}), measured by 4-nitrophenylboronic acid (NPBA) assay. (b) Concentration of PANs in SOA, [PAN]$_m$ (nmol μg^{-1}), measured by Griess assay. The number above each column represents the initial HC/NO$_x$ ratio. The *x*-axis represents the mid-collection time (Table 1). (c) Comparison of DTT$_m$ (*t* = 2 h) with the sum of [OHP]$_m$ and [PAN]$_m$. The [OHP]$_m$, [PAN]$_m$, and DTT$_m$ are expressed as the mean (± σ) of three replicates. HNOX represents high NO$_x$ conditions, and LNOX represents low NO$_x$ conditions.
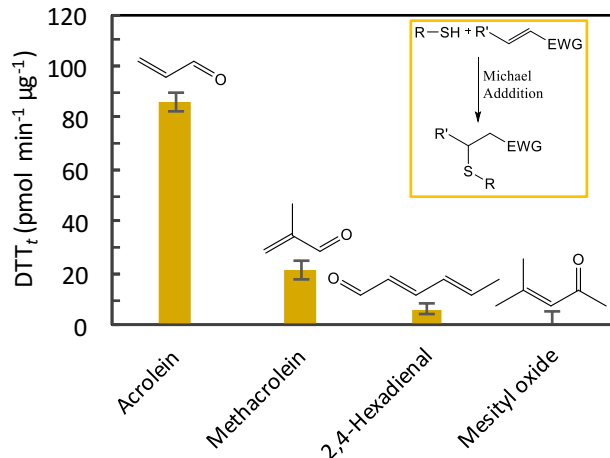
Figure 6. The DTT$_t$ (*t* = 30 min) of four different electron-deficient alkenes. Each error bar was calculated by $t_{0.95} \times \sigma / \sqrt{n}$ using three replicates, where $t_{0.95}$ is the t-score (4.303 for *n* = 3 replicates) with a two-tail 95 % confidence level. EWG appeared in the mechanism represents an electron withdrawing group (Nair et al., 2014).